DOI: 10.1002/ejic.201000348

Chromophoric Lewis Base Adducts of Methyltrioxorhenium: Synthesis, Catalysis and Photochemistry

Simone A. Hauser,[a] Valentina Korinth,[b] Eberhardt Herdtweck,[a] Mirza Cokoja,[a] Wolfgang A. Herrmann,[a] and Fritz E. Kühn*[a,b]

Keywords: Rhenium / Homogeneous catalysis / Photochemistry / Epoxidation / Stability constants

A series of chromophoric Lewis base adducts of methyltrioxorhenium (MTO) was examined. The ligands were pyridine derivatives with different size of the aromatic system and variable substituents, thus providing a variation of electronic and steric parameters. The complexes were fully characterised (UV/Vis, IR and NMR spectroscopy, single-crystal X-ray diffraction and elemental analysis) and their stability constants in dichloromethane were determined by means of UV/Vis spectroscopy. Moreover, this report presents a study of the influence of these N-donor ligands coordinated to MTO on the catalytic activity of epoxidation of 1-octene. Each compound was tested twice; in a catalytic reaction under exclusion of light and in daylight. No significant differences in catalytic performance were found. The behaviour of the complexes under irradiation with UV light was investigated by means of ^{17}O-NMR and UV/Vis spectroscopy. The herein exposed experiments aimed for probing potential beneficial effects of chromophoric N-donor ligands in MTO adducts, as they might activate the catalytic system by providing additional energy for weakening bonds that have to be broken during the catalytic cycle.

Introduction

Much research has been dedicated to the chemistry of methyltrioxorhenium (MTO) since its discovery by Beattie and Jones[1] in the late 1970s and the improvement of the synthesis by Herrmann and co-workers[2] some years later. The latter group discovered the ability of MTO to act as a versatile catalyst of various organic reactions.[3] MTO can be used in several catalytic processes, for instance olefin metathesis[4] and aldehyde olefination.[5] Most recently, MTO has been successfully applied in deoxygenation of epoxides.[6] However, the most important and thus best studied MTO-catalysed reaction is olefin epoxidation.[7–9] Due to the strong Lewis acidity of the metal centre, undesired side reactions such as ring opening and diol formation are usually occurring. This can be prevented by addition of bases, mostly pyridine, bipyridine or pyrazole and their derivatives, as shown by Sharpless et al. and other groups.[8,10–19] The photochemistry of MTO was for the first time under examination in the early 1990s.[20,21] MTO solutions were found to be very sensitive to UV light, the rhenium-carbon bond was reported to be photolysed after a short irradiation time, with subsequent formation of ReO_4^- and ReO_3, at low and high concentrations.[20] Some years later, the studies were extended to Lewis base adducts of MTO. Interesting properties of these adducts were published,[22,23] but no further research was conducted in this direction. This prompted us to investigate the effect of a number of novel chromophoric Lewis base adducts of MTO with respect to the complex stability under irradiation with UV light.

[a] Chair of Inorganic Chemistry, Catalysis Research Center, Technische Universität München,
Lichtenbergstrasse 4, 85748 Garching, Germany
Fax: +49-89-289-13473
E-mail: fritz.kuehn@ch.tum.de
[b] Molecular Catalysis, Catalysis Research Center, Technische Universität München,
Lichtenbergstrasse 4, 85748 Garching, Germany
Supporting information for this article is available on the WWW under http://dx.doi.org/10.1002/ejic.201000348.

Results and Discussion

Synthesis and Spectroscopic Characterisation

A series of chromophoric pyridine derivatives (**1**–**7**, Figure 1) was synthesised and the coordination to MTO was

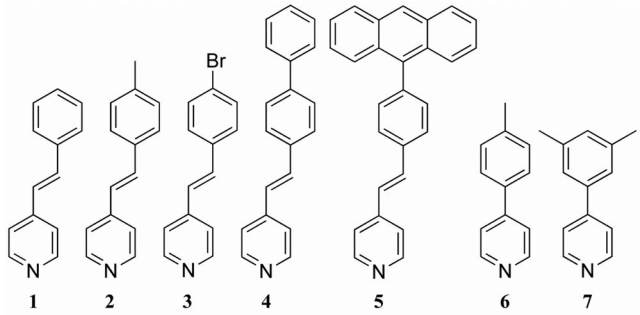

Figure 1. Overview of the pyridine derivatives employed as ligands for coordination to MTO.

examined. Complexes **8**–**14** were formed by treatment of MTO with ligands **1**–**7** in a 1:1 ratio in diethyl ether at room temperature (Scheme 1). Subsequent cooling of the yellow solution led to precipitation of yellow crystals, which were isolated by filtration and purified by washing with *n*-hexane. The compounds obtained are stable to air, both in the solid state and in dichloromethane solution.

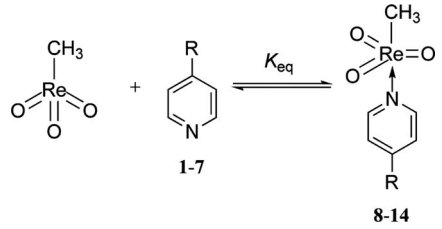

Scheme 1. Adduct formation of MTO with pyridine derivatives in solution.

Selected ^{1}H and ^{13}C NMR spectroscopic data of compounds **8**–**14** are shown in Table 1. The proton signals of the MTO methyl group of the complexes are considerably shifted to higher field, indicating the strength of the Re–N bond.[15] The same effect is observed in the ^{13}C NMR spectra. The vicinal protons to the nitrogen of the ligand have a different electronic environment, similar to the methyl group of the MTO, which is manifested by a high-field shift compared to the free ligand.

Table 1. Selected ^{1}H and ^{13}C NMR spectroscopic data for complexes **8**–**14** in $CDCl_3$.

	α-H ligand, ^{1}H δ [ppm]	α-H adduct ^{1}H, δ [ppm]	Re-C*H*$_3$, ^{1}H δ [ppm]	Re-*C*H$_3$, ^{13}C δ [ppm]
MTO	–	–	2.67	19.0
8	8.51 (**1**)	8.29	2.03	24.7
9	8.55 (**2**)	8.20	1.92	25.1
10	8.58 (**3**)	8.26	1.96	24.0
11	8.59 (**4**)	8.34	2.13	24.4
12	8.63 (**5**)	8.33	2.00	24.9
13	8.63 (**6**)	8.31	1.97	24.8
14	8.65 (**7**)	8.32	1.98	24.4

In the IR spectra, a red-shift of Re = O bands compared to free MTO is observable. This gives rise to an enhanced electron density donated from the ligand to the Re centre, causing weakening of the Re=O bond (see Table 2).

Table 2. Characteristic IR vibrations of CH_3ReO_3 fragments (cm^{-1}) in **8**–**14**.

MTO	**8**	**9**	**10**	**11**	**12**	**13**	**14**	Assignment
998	934	936	931	n.o.	n.o.	934	931	ReO_3 sym str.
965	927	926	n.o.[a]	927	928	927	n.o.	ReO_3 asym str.

[a] Not observed.

X-ray Crystal Structure of Ligand 5 and Complexes 8–14

The solid-state structure of the synthesised compounds **5** and **8**–**14** was measured; one example is shown in Figure 2. Selected bond lengths are given in Table 3. With one exception (compound **11**), the N-base ligand coordinates *trans* to the methyl group to the rhenium centre. Complex **11**, however, exists in both *cis* and *trans* arrangements in the solid state. Together with the finding that only one peak is visible in the ^{17}O-NMR spectrum, this strongly indicates that packing forces are responsible for the solid-state configuration, rather than electronic or steric ligand effects. Moreover, this conclusion is in accordance with previously reported data.[24]

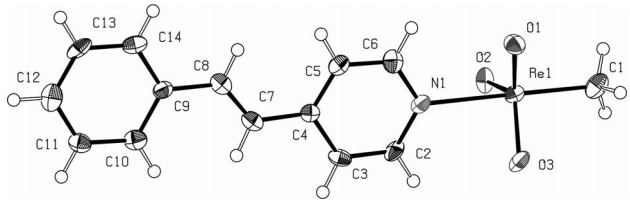

Figure 2. PLATON view of the solid-state structure of complex **8**. The thermal ellipsoids are shown at the 50% probability level.

Table 3. Selected bond lengths for complexes **8**–**14** (*trans* configuration) determined by single-crystal X-ray diffraction.

	Re–N [Å]	Re–C [Å]	Re–O [Å]
MTO[a]	–	2.074(4)	1.703(2)
8	2.422(5)	2.113(7)	1.712(3) 1.706(6) 1.726(7)
9	2.445(5)	2.094(6)	1.718(4) 1.705(4) 1.707(4)
10[b]	2.439(4)	2.099(5)	1.717(4) 1.716(3) 1.716(3)
	2.438(5)	*2.102(6)*	*1.711(3) 1.716(4) 1.720(3)*
11[b]	2.372(3)	2.112(4)	1.722(3) 1.719(3) 1.713(3)
	2.439(3)	*2.081(5)*	*1.714(3) 1.712(3) 1.714(3)*
12	2.418(2)	2.091(3)	1.720(2) 1.711(2) 1.714(2)
13	2.417(3)	2.092(4)	1.716(4) 1.716(3) 1.722(3)
14[b]	2.408(4)	2.102(5)	1.713(2) 2×1.708(4)
	2.392(4)	*2.101(5)*	*1.706(3) 2×1.694(4)*

[a] Values taken from ref.[25]. [b] The values of the second crystallographically independent molecule are printed in *italics*.

Determination of Formation Constants

The formation constants of the MTO – ligand adducts **8**–**14** were determined by means of UV/Vis spectroscopy.[26] Scheme 1 shows the equilibrium that is established in presence of MTO and a pyridine derivative. According to Equation (1), which is derived from the Lambert–Beer law (path length: 1 cm), the absorbance of the solution (*Abs*) changes in function of the presence of free ligand (L), uncoordinated MTO (M) and the MTO-ligand adduct (ML).

$$Abs = \varepsilon_L[L] + \varepsilon_M[M] + \varepsilon_{ML}[ML] \quad (1)$$

The adduct concentration [ML] can be expressed using the formation constant (K_{eq}) by taking into account the molar balance $[M]_T = [M] + [ML]$, leading to Equation (2).

$$Abs = \varepsilon_L[L] + \varepsilon_M[M] + \frac{\varepsilon_{ML}[M]_T \cdot K_{eq}[L]}{1 + K_{eq}[L]} \quad (2)$$

Above 330 nm, the absorbance of MTO is negligible, i.e. $\varepsilon_M \approx 0$.[27] If the absorbance of the free ligands at the chosen wavelength can also be ignored, i.e. $\varepsilon_L \approx 0$, then Equation (3) can be used to calculate the formation constant.

$$Abs = \frac{\varepsilon_{ML}[M]_T \cdot K_{eq}[L]}{1 + K_{eq}[L]} \quad (3)$$

The values of the adduct formation constants (Table 4) are calculated by fitting of experimental absorbance data to Equation (2) or (3). Figure 3 shows the change in the absorption spectrum upon successive addition of MTO to a ligand solution in CH_2Cl_2. In the case of the compound **10**, complex formation can be noticed at 350 nm. Thus, the values at this wavelength have been used for the curve fitting according to Equation (3) (see Figure 4).

Table 4. Formation constants of compounds **8**–**14** in CH_2Cl_2.

	Absorbance [nm]	Formation constant (K_{eq}) [L mol^{-1}]
8	340	431 ± 27
9	355	563 ± 88
10	350	386 ± 47
11	370	309 ± 36
12	335	78 ± 25
13	300	348 ± 93
14	300	286 ± 98

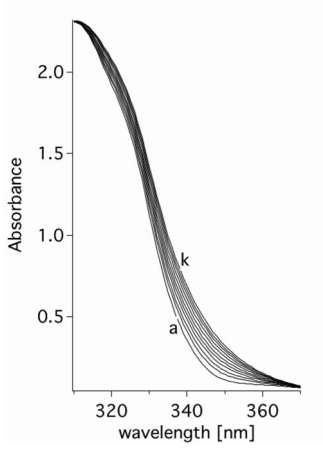

Figure 3. Change in the absorption in function of complex formation (**10**). (a) free ligand ([**3**] = 0.1 mM), successive addition of 1 equiv. of MTO, (k) ligand with 10 equiv. MTO.

The values of the formation constants for complexes **8**–**14** are comparable to those reported in literature.[26,28–30] Moreover, the influence of both the electronic and steric nature of the ligand can be seen. The stability of the adducts is higher when the ligand has electron-donating substituents and is less sterically crowded. The electronic effect is nicely seen when comparing the formation constant of complex **9** with that of complex **10**. The steric effect accounts for the difference in the value of the formation constant of complex **13** and complex **14**.

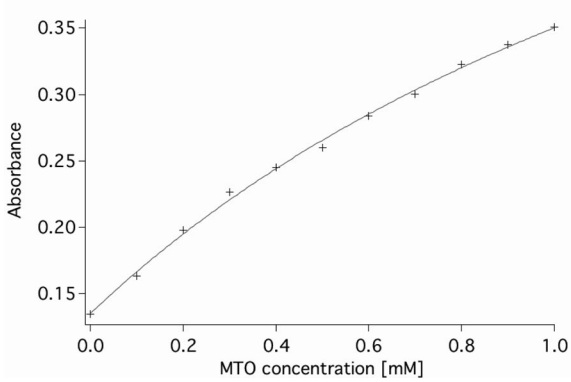

Figure 4. Curve fitting with Equation 3 for determination of formation constant of complex **10**.

Application in Epoxidation Catalysis

The performance of ligands **2**–**7** was tested in the MTO-catalysed epoxidation of 1-octene with hydrogen peroxide. *tert*-Butylpyridine (*t*Bu-Pyr) was chosen as a benchmark ligand. A catalyst:ligand:oxidant:substrate ratio of 1:5:150:100 was used in all experiments, unless stated otherwise. The catalytic tests were performed at room temperature and twice with each ligand: once with exclusion of light and once in light with the goal to establish a statement about the supposed beneficial effect of chromophoric pyridine derivatives with respect to the already known advantages of simple pyridine derivatives in epoxidation catalysis with MTO.[19] Further details are given in the Exp. Section. No significant diol formation or formation of other by-products could be observed.

Table 5 summarises the turnover frequencies (TOF) of the different catalytic systems tested. Maximum epoxide yield is obtained after 24 h reaction time, with a substrate conversion between 50 and 80% (Figure 5). *t*Bu-Pyr shows no significant advantage in catalytic performance compared to the chromophoric pyridine derivatives. Moreover, it can be noted that the advantage of running the catalytic reaction under exclusion of light is negligible with either type of pyridine ligand. The yields of 1-octene epoxide with the ligand additives tested within this work are comparable to

Table 5. Turnover frequencies [mol(epoxide) mol(cat)$^{-1}$ h^{-1}] determined after 5 min.

Ligand	TOF [h^{-1}]	Yield [%], after 24 h with exclusion of light
2	63	76
3	44	69
4	65	69
5	46	65
6	49	73
7	41	72
*t*Bu-Pyr	35	71

the yield achieved with MTO alone.[31] Nevertheless, they are far from those obtained with 3-methylpyrazole or pyrazole under the same conditions.[31]

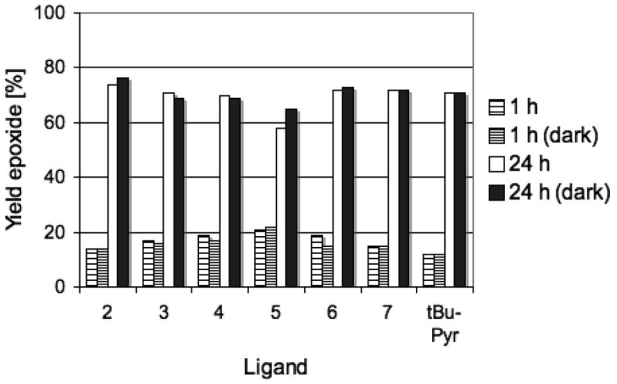

Figure 5. 1-Octene epoxide yields with different ligands.

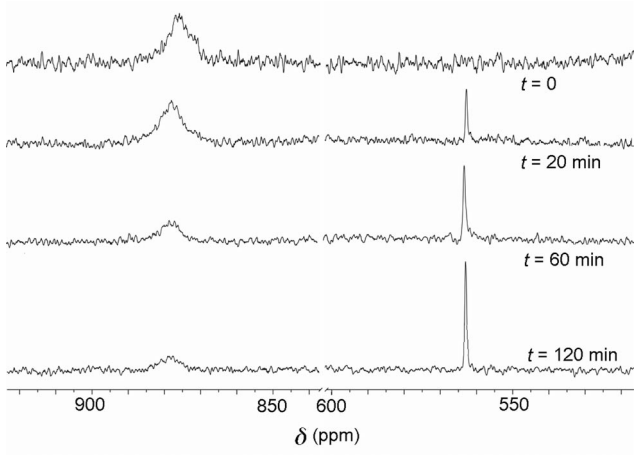

Figure 6. Time resolved ^{17}O-NMR spectra of complex **11** before (top) and after irradiation with UV light. The signal of the MTO oxo moieties at δ = 879 ppm is broadened due to fluxional equilibrium of complex formation, whereas the sharp peak at δ = 563 ppm can be assigned [ReO_4^-].

Photostability of the Synthesised Compounds

One aim of this work is to probe potential beneficial effect of chromophoric Lewis bases in MTO adducts. They might activate the catalytic system by providing additional energy for weakening bonds that have to be broken during the catalytic cycle. However, photoinduced homolysis of the Re–CH_3 bond in solution is the most common way of degradation of MTO.[20] Vogler et al. reported the photoassisted isomerisation of 4-styrylpyridine, where the complex remained intact, i.e. the MTO was not affected by UV-radiation.[23] This led to the hypothesis that larger chromophoric systems might lead to stable MTO Lewis base adducts on the one hand, and act as a photosensitisers on the other hand. The most convenient approaches to study the stability or the photo-induced degradation of the MTO adducts are ^{17}O-NMR and UV/Vis spectroscopy.

For the NMR studies, a 0.1 M solution of the complexes in $CDCl_3$ was used and treated with UV light (λ = 368 nm). In a second experiment, a fivefold excess of ligand was added to MTO, in order to mimic the reaction conditions of the catalytic tests (vide supra). The chemical shift of the oxygen atoms of the freshly synthesised complexes was found to be between 865 ppm and 885 ppm which is consistent with the reported literature values.[32,33] Upon irradiation, already after 6 min a peak at δ = 563 ppm was detected, which could be attributed to the perrhenate anion.[32] This peak became more pronounced after longer irradiation time (see Figure 6). There was no significant difference in stability of the MTO in the two experiments performed. Noteworthy, all complexes synthesised in this work have shown the same behaviour under irradiation with UV light (see Supporting Information).

The UV/Vis spectra were recorded in CH_2Cl_2. A 0.1 M solution of selected complexes was irradiated with UV light and several samples were taken. Figure 7 shows the spectral change over a time span of 2 h. Ligand absorption is very strong, it shows a maximum at 325 nm. It partially overlaps complex absorption as well as the absorbance pattern of free MTO.[20] Upon photolytic degradation of MTO, the ligand is protonated. Thus, its absorbance spectrum changes by a shift of the maximum to 375 nm.

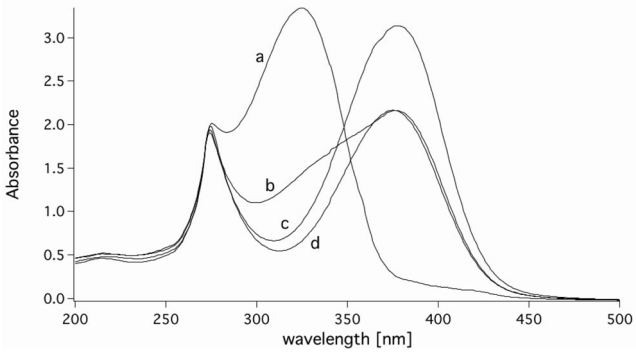

Figure 7. UV/Vis spectra of complex **11** in CH_2Cl_2 (c = 0.16 mM). (a) Initial spectrum; (b) after 20 min exposure to UV light; (c) after 60 min; (d) after 120 min, the decrease in intensity of the peak at 377 nm can be explained by precipitation of the perrhenate and protonated ligand.

The above-mentioned experiments clearly show that both the MTO and the ligands are affected by prolonged irradiation with UV light. Thus, no additional stability is brought to the adducts by the use of chromophoric pyridine derivatives. Despite of the use of chromophoric pyridine derivatives as ligands on MTO, the obtained adducts are not stable to UV light. However, as described above, the catalytic epoxidation is not influenced by light.

Conclusions

In this study, seven chromophoric pyridine derivatives were prepared and treated with MTO to form seven Lewis base adducts of MTO. They have been fully characterised and tested as catalysts in the epoxidation of 1-octene with

H_2O_2. With respect to the benchmark ligand *tert*-butylpyridine, the presented ligands do not show any advantages in the epoxidation of 1-octene, whether performed under exclusion of light or in daylight (see Figure 5). Moreover, the photochemistry of the complexes was studied by means of UV/Vis and ^{17}O-NMR spectroscopy. The chromophoric ligands did not influence the adduct stability under UV irradiation. Complex decomposition occurred through the reported pathway,[20] as formation of the perrhenate anion was already observable after a short irradiation time with UV light (see Figure 6 and Figure 7).

Experimental Section

Materials and Methods: All experimental work was carried out using standard Schlenk techniques under argon. Solvents were dried by standard procedures (hexane and diethyl ether over Na/benzophenone; CH_2Cl_2 over CaH_2), distilled and stored under argon over molecular sieves. High resolution NMR spectra were measured with Bruker Avance DPX-400 (^{1}H: 400 MHz; ^{13}C: 100.6 MHz; ^{17}O: 54.2 MHz), and JEOL NMR GX-400 (^{1}H: 400 MHz; ^{13}C: 100.6 MHz) spectrometers. The UV/Vis spectra were recorded on a JASCO UV/Vis V-550 spectrophotometer and the IR spectra on a Perkin–Elmer 1600 series FT-IR instrument. Microanalyses of the obtained products were performed in the Mikroanalytisches Labor of the Technical University of Munich, Garching, Germany. MTO was synthesised according to literature procedures.[34]

Ligand Synthesis: Ligands **1**–**3** were synthesised by treating a solution of 4-picoline (2.48 mmol) in THF at –60 °C with an equimolar amount of lithium diisopropylamine in THF.[35] The alcoholate was formed upon addition of the corresponding aldehyde, which was subsequently eliminated by refluxing in concentrated acetic acid for 18 h to form the C–C double bond. Purification was done by column chromatography on silica gel. The synthesis of ligands **4**–**7** was based on the Suzuki cross coupling mechanism described by Fu et al.[36] The heteroaryl boronic acid reacted with an aryl bromide in refluxing dioxane, whereas the reaction was catalysed by $[Pd_2(dba)_3]$ (dba = dibenzylideneacetone), PCy_3 and K_3PO_4 (aq.). Subsequent purification steps included filtration, extraction of the filtrate and column chromatography.

4-Styrylpyridine (1): Yield 314 mg (70%). ^{1}H NMR (400 MHz, $CDCl_3$, 25 °C): δ = 8.51 [d, J(H,H) = 4.8 Hz, 2 H, $NC_2H_2C_2H_2C$-], 7.48 [d, J(H,H) = 7.4 Hz, 2 H, -$CC_2H_2C_2H_2CH$], 7.35–7.24 (m, 4 H, $NC_2H_2C_2H_2C$-CHCH-$CC_2H_2C_2H_2CH$), 7.21 [d, J(H,H) = 9.8 Hz, 2 H, -$CC_2H_2C_2H_2CH$], 6.96 [d, J(H,H) = 15.9 Hz, 1 H, Pyr-CHCH-Ph] ppm. ^{13}C NMR (100.6 MHz, $CDCl_3$, 25 °C): δ = 150.2 (2 C), 144.6 (2 C), 136.2 (1 C), 133.2 (1 C), 128.8 (2 C), 128.7 (2 C), 127.0 (1 C), 126.0 (2 C), 120.8 (1 C) ppm.

4-[2-(4-Methylphenyl)ethenyl]pyridine (2): Yield 386 mg (80%). ^{1}H NMR (400 MHz, $CDCl_3$, 25 °C): δ = 8.55 [d, J(H,H) = 6.0 Hz, 2 H, $NC_2H_2C_2H_2C$-], 7.43 [d, J(H,H) = 8.0 Hz, 2 H, $NC_2H_2C_2H_2C$-], 7.34 [d, J(H,H) = 6.0 Hz, 2 H, -$CC_2H_2C_2H_2CCH_3$], 7.27 [d, J(H,H) = 13.6 Hz, 1 H, -PhCHCHPyr-], 7.18 [d, J(H,H) = 7.6 Hz, 2 H, -$CC_2H_2C_2H_2CCH_3$], 6.95 [d, J(H,H) = 16.0 Hz, 1 H, -PhCHCHPyr-], 2.37 (s, 3 H, -$CC_2H_2C_2H_2CCH_3$) ppm. ^{13}C NMR (100.6 MHz, $CDCl_3$, 25 °C): δ = 150.2 (1 C, $NC_2H_2C_2H_2C$-), 144.8 (2 C, $NC_2H_2C_2H_2C$-), 138.9 (1 C, -$CC_2H_2C_2H_2CCH_3$), 133.4 (1 C, -$CC_2H_2C_2H_2CCH_3$), 133.1 (1 C, -PhCHCHPyr-), 129.5 (2 C, -$CC_2H_2C_2H_2CCH_3$), 126.9 (2 C, -$CC_2H_2C_2H_2CCH_3$), 124.9 (1 C, -PhCHCHPyr-), 120.8 (2 C, $NC_2H_2C_2H_2C$-), 21.3 (1 C, -PhCH$_3$) ppm.

4-[2-(4-Bromophenyl)ethenyl]pyridine (3): Yield 503 mg (78%). ^{1}H NMR (400 MHz, $CDCl_3$, 25 °C): δ = 8.58 [d, J(H,H) = 6.0 Hz, 2 H, $NC_2H_2C_2H_2C$-], 7.50 [d, J(H,H) = 8.4 Hz, 2 H, -$CC_2H_2C_2H_2CBr$], 7.38 [d, J(H,H) = 8.4 Hz, 2 H, -$CC_2H_2C_2H_2CBr$], 7.34 [J(H,H) = 5.2 Hz, 2 H, $NC_2H_2C_2H_2C$-], 7.22 [d, J(H,H) = 16.4 Hz, 1 H, PyrCHCH-], 6.98 [d, J(H,H) = 16.4 Hz, 1 H, PyrCHCH-] ppm. ^{13}C NMR (100.6 MHz, $CDCl_3$, 25 °C): δ = 150.30 (2 C, N$C_2H_2C_2H_2C$-), 144.23 (1 C, $NC_2H_2C_2H_2C$-), 135.13 (1 C, -$CC_2H_2C_2H_2CBr$), 132.02 (2 C, -$CC_2H_2C_2H_2CBr$), 131.87 (1 C, PyrCHCH-), 128.44 (2 C, -$CC_2H_2C_2H_2CBr$), 126.76 (1 C, Pyr$C$HCH-), 122.68 (1 C, -$CC_2H_2C_2H_2CBr$), 120.85 (2 C, $NC_2H_2C_2H_2C$-) ppm.

4-[2-(Biphenyl)ethenyl]pyridine (4): Yield 980 mg (83%). ^{1}H NMR (400 MHz, $CDCl_3$, 25 °C): δ = 8.59 [d, J(H,H) = 8.0 Hz, 2 H, $NC_2H_2C_2H_2C$-], 7.63 (m, 7 H, -$CC_2H_2C_2H_2C$-$CC_2H_2C_2H_2CH$), 7.46 [t, J(H,H) = 8.0 Hz, 2 H, -$CC_2H_2C_2H_2CH$], 7.39 (m, 2 H, $NC_2H_2C_2H_2C$-), 7.35 [d, J(H,H) = 16.0 Hz, 1 H, Pyr-CHCH-Ph-Ph], 7.06 [d, J(H,H) = 16.0 Hz, 1 H, Pyr-CHCH-Ph-Ph] ppm. ^{13}C NMR (100.6 MHz, $CDCl_3$, 25 °C): δ = 150.20 (2 C, N$C_2H_2C_2H_2C$-), 144.62 (1 C, $NC_2H_2C_2H_2C$-), 141.51 (1 C, -$CC_2H_2C_2H_2CH$), 140.38 (1 C, -$CC_2H_2C_2H_2C$-$CC_2H_2C_2H_2CH$), 135.16 (1 C, -$CC_2H_2C_2H_2C$-$CC_2H_2C_2H_2CH$), 132.71 (1 C, Pyr-CHCH-Ph-Ph), 128.85 (2 C, -$CC_2H_2C_2H_2CH$), 127.58 (1 C, -$CC_2H_2C_2H_2CH$), 127.47 (4 C, -$CC_2H_2C_2H_2C$-C$C_2H_2C_2H_2CH$), 126.95 (2 C, -C$C_2H_2C_2H_2C$-$CC_2H_2C_2H_2CH$), 125.99 (1 C, Pyr-CHCH-Ph-Ph), 120.83 (2 C, $NC_2H_2C_2H_2C$-) ppm.

4-[2-(4-Anthracenylphenyl)ethenyl]pyridine (5): Yield 880 mg (65%). ^{1}H NMR (400 MHz, $CDCl_3$, 25 °C): δ = 8.63 [d, J(H,H) = 4.9 Hz, 2 H], 8.52 (s, 1 H), 8.06 [d, J(H,H) = 8.6 Hz, 2 H], 7.77 [d, ^3J(H,H) = 8.6 Hz, 2 H], 7.69 [d, J(H,H) = 8.6 Hz, 2 H], 7.47 [t, J(H,H) = 8.6, 7.4 Hz, 7 H], 7.37 [t, ^3J(H,H) = 7.4, 7.4 Hz, 2 H], 7.18 [d, J(H,H) = 15.9 Hz, 1 H] ppm. ^{13}C NMR (100.6 MHz, $CDCl_3$, 25 °C): δ = 150.2 (2 C), 144.7 (1 C), 139.5 (1 C), 136.3 (1 C), 135.4 (1 C), 132.9 (1 C), 131.8 (2 C), 131.4 (2 C), 130.1 (2 C), 128.4 (1 C), 127.0 (3 C), 126.8 (1 C), 126.6 (2 C), 126.3 (2 C), 125.5 (1 C), 125.1 (2 C), 120.9 (2 C) ppm.

4-Tolylpyridine (6): Yield 193 mg (60%). ^{1}H NMR (400 MHz, $CDCl_3$, 25 °C): δ = 8.63 [d, J(H,H) = 5.4 Hz, 2 H, $NC_2H_2C_2H_2C$-], 7.53 [d, J(H,H) = 8.0 Hz, 2 H, $NC_2H_2C_2H_2C$-], 7.48 [d, J(H,H) = 6.0 Hz, 2 H, -$CC_2H_2C_2H_2CCH_3$], 7.28 [d, J(H,H) = 8.0 Hz, 2 H, -$CC_2H_2C_2H_2CCH_3$], 2.40 (s, 3 H, -PhCH_3) ppm. ^{13}C NMR (100.6 MHz, $CDCl_3$, 25 °C): δ = 150.2 (2 C, N$C_2H_2C_2H_2C$-), 148.2 (1 C, $NC_2H_2C_2H_2C$-), 139.2 [1 C, -$CC_2H_2C_2H_2C(CH_3)$], 135.2 [1 C, -$CC_2H_2C_2H_2C(CH_3)$], 129.8 [2 C, -$CC_2H_2C_2H_2C(CH_3)$], 126.8 [2 C, -C$C_2H_2C_2H_2C(CH_3)$], 121.4 (2 C, $NC_2H_2C_2H_2C$-), 21.2 (1 C, -PhCH$_3$) ppm.

4-(3,5-Dimethylphenyl)pyridine (7): Yield 450 mg (66%). ^{1}H NMR (400 MHz, $CDCl_3$, 25 °C): δ = 8.65 [d, J(H,H) = 6.8 Hz, 2 H, $NC_2H_2C_2H_2C$-], 7.50 [d, J(H,H) = 6.8 Hz, 2 H, $NC_2H_2C_2H_2C$-], 7.27 [s, 2 H, -$CC_2H_2C_2(CH_3)_2CH$], 7.10 [s, 1 H, -$CC_2H_2C_2(CH_3)_2CH$], 2.41 [s, 6 H, -$CC_2H_2C_2(CH_3)_2CH$] ppm. ^{13}C NMR (100.6 MHz, $CDCl_3$, 25 °C): δ = 150.15 (2 C, N$C_2H_2C_2H_2C$-), 148.65 (1 C, $NC_2H_2C_2H_2C$-), 138.71 [2 C, -$CC_2H_2C_2(CH_3)_2CH$], 138.18 [1 C, -$CC_2H_2C_2(CH_3)_2CH$], 130.67 [1 C, -$CC_2H_2C_2(CH_3)_2CH$], 124.86 [2 C, -C$C_2H_2C_2(CH_3)_2CH$], 121.69 (2 C, $NC_2H_2C_2H_2C$-), 21.36 [2 C, -$CC_2H_2C_2(CH_3)_2CH$] ppm.

Typical Procedure for the Preparation of the Chromophoric Lewis Base Adducts of MTO: An equimolar amount of MTO and ligand was dissolved in diethyl ether and the solution was stirred for 1 h

before cooling the mixture in an ice bath. A yellow precipitate formed, which was filtered and washed with hexane. The solid was dried in vacuo and analysed by standard analysis methods.

Methyl(4-styrylpyridine)trioxorhenium (8): Yield 58 mg (76%). ^{1}H NMR (400 MHz, $CDCl_3$, 25 °C): δ = 8.29 [d, J(H,H) = 6.2 Hz, 2 H, $NC_2H_2C_2H_2C$-], 7.54 [d, J(H,H) = 7.4 Hz, 2 H, -$CC_2H_2C_2H_2CH$], 7.45 (m, 6 H, $NC_2H_2C_2H_2C$-CHCH-$CC_2H_2C_2H_2CH$), 7.01 [d, J(H,H) = 17.2 Hz, 1 H, Pyr-CHCH-Ph], 2.03 (s, 3 H, -ReCH_3) ppm. ^{13}C NMR (100.6 MHz, $CDCl_3$, 25 °C): δ = 147.2 (2 C), 135.6 (2 C), 135.5 (1 C), 129.3 (1 C), 128.9 (2 C), 127.3 (2 C), 124.7 (1 C), 121.9 (2 C), 24.7 (1 C) ppm. IR (KBr): $\tilde{\nu}$ = 1605 (vs), 1499 (w), 1449 (w), 1428 (w), 1384 (w), 1013 (m), 971 (m), 961 (w), 934 (vs), 927 (vs), 877 (w), 818 (m), 559 (w), 548 (m) cm^{-1}. $C_{14}H_{14}NO_3Re$ (430.47): calcd. C 39.06, H 3.28, N 3.25; found C 39.56, H 3.31, N 3.34.

Methyl{4-[2-(4-Methylphenyl)ethenyl]pyridine}trioxorhenium (9): Yield 53 mg (72%). ^{1}H NMR (400 MHz, $CDCl_3$, 25 °C): δ = 8.20 [d, J(H,H) = 5.4 Hz, 2 H, $NC_2H_2C_2H_2C$-], 7.42 (m, 4 H, $NC_2H_2C_2H_2C$-, -$CC_2H_2C_2H_2CCH_3$), 7.30 [d, J(H,H) = 16.2 Hz, 1 H, -PhCHCHPyr-], 7.20 [d, J(H,H) = 7.9 Hz, 2 H, -$CC_2H_2C_2H_2CCH_3$], 6.93 [d, J(H,H) = 16.2 Hz, 1 H, -PhCHCHPyr-], 2.37 (s, 3 H, -PhCH_3), 1.92 (s, 3 H, -ReCH_3) ppm. ^{13}C NMR (100.6 MHz, $CDCl_3$, 25 °C): δ = 147.94 (1 C, $NC_2H_2C_2H_2C$-), 147.06 (2 C, N$C_2H_2C_2H_2C$-), 139.66 (1 C, -$CC_2H_2C_2H_2C$$CH_3$), 135.48 (1 C, -$C$$C_2H_2C_2H_2CCH_3$), 132.76 (1 C, -Ph$C$HCHPyr-), 129.65 (2 C, -$CC_2H_2C_2H_2CCH_3$), 127.23 (2 C, -$CC_2H_2C_2H_2CCH_3$), 123.52 (1 C, -PhCH$C$HPyr-), 121.85 (2 C, $NC_2H_2C_2H_2C$-), 25.08 (1 C, -ReCH_3), 21.36 (1 C, -PhCH_3) ppm. IR (KBr): $\tilde{\nu}$ = 3434 (w), 3025 (w), 1636 (m), 1602 (vs), 1514 (m), 1428 (m), 1384 (w), 1210 (w), 1183 (w), 1013 (s), 975 (m), 936 (vs), 926 (vs), 826 (s), 736 (w), 706 (w), 624 (m), 547 (s), 502 (m) cm^{-1}. $C_{15}H_{16}NO_3Re$ (444.50): calcd. C 40.53, H 3.63, N 3.15; found C 38.55, H 3.33, N 3.16.

{4-[2-(4-Bromophenyl)ethenyl]pyridine}methyltrioxorhenium (10): Yield 68 mg (79%). ^{1}H NMR (400 MHz, $CDCl_3$, 25 °C): δ = 8.26 [d, J(H,H) = 6.2 Hz, 2 H, $NC_2H_2C_2H_2C$-], 7.52 [d, J(H,H) = 8.3 Hz, 2 H, -$CC_2H_2C_2H_2CBr$], 7.41 (m, 4 H, $NC_2H_2C_2H_2C$-, -$CC_2H_2C_2H_2CBr$), 7.25 [d, J(H,H) = 16.4 Hz, 1 H, Pyr-CHCH-], 6.98 [d, J(H,H) = 16.2 Hz, 1 H, Pyr-CHCH-], 1.96 (s, 3 H, -ReCH_3) ppm. ^{13}C NMR (100.6 MHz, $CDCl_3$, 25 °C): δ = 147.3 (2 C), 147.0 (1 C), 134.5 (1 C), 134.1 (1 C), 132.1 (3 C), 128.7 (2 C), 125.4 (1 C), 123.5 (1 C), 122.0 (1 C), 24.0 (1 C) ppm. IR (KBr): $\tilde{\nu}$ = 3466 (w), 3048 (w), 2973 (w), 1895 (w), 1773 (w), 1637 (m), 1610 (vs), 1586 (s), 1497 (m), 1483 (m), 1428 (s), 1393 (m), 1385 (m), 1209 (m), 1070 (vs), 1017 (vs), 1008 (s), 975 (s), 970 (s), 928 (vs), 883 (m), 875 (m), 829 (vs), 738 (w), 674 (w), 583 (m), 557 (s), 542 (s). 496 (w) cm^{-1}. $C_{14}H_{13}BrNO_3Re$ (509.37): calcd. C 33.01, H 2.57, N 2.75; found C 32.88, H 2.53, N 2.78.

{4-[2-(Biphenyl)ethenyl]pyridine}methyltrioxorhenium (11): Yield 69 mg (80%). ^{1}H NMR (400 MHz, $CDCl_3$, 25 °C): δ = 8.34 [d, J(H,H) = 6.2 Hz, 2 H, $NC_2H_2C_2H_2C$-], 7.62 (m, 6 H, -$CC_2H_2C_2H_2C$-$CC_2H_2C_2H_2CH$), 7.47–7.37 (m, 5 H, $NC_2H_2C_2H_2C$-, -$CC_2H_2C_2H_2CH$), 7.36 [d, J(H,H) = 16.2 Hz, 1 H, Pyr-CHCH-Ph-Ph], 7.04 [d, J(H,H) = 16.2 Hz, 1 H, Pyr-CHCH-Ph-Ph], 2.13 (s, 3 H, -ReCH_3) ppm. ^{13}C NMR (100.6 MHz, $CDCl_3$, 25 °C): δ = 147.7 (2 C), 147.0 (1 C), 142.0 (1 C), 140.2 (1 C), 140.2 (1 C), 134.6 (2 C), 128.9 (2 C), 127.7 (2 C), 127.6 (2 C), 127.0 (2 C), 124.8 (1 C), 121.7 (2 C), 24.4 (1 C) ppm. IR (KBr): $\tilde{\nu}$ = 344 (w), 3032 (w), 1600 (s), 1487 (m), 1426 (m), 1204 (w), 1195 (w), 1015 (m), 976 (m), 934 (vs), 927 (vs), 879 (w), 836 (m), 765 (m), 737 (w), 690 (m), 638 (w), 561 (m), 529 (w) cm^{-1}. $C_{20}H_{18}NO_3Re$ (506.57): calcd. C 47.40, H 3.58, N 2.77; found C 47.33, H 3.58, N 2.77.

{4-[2-(4-Anthracenylphenyl)ethenyl]pyridine}methyltrioxorhenium (12): Yield 87 mg (84%). ^{1}H NMR (400 MHz, $CDCl_3$, 25 °C): δ = 8.51 (s, 1 H), 8.33 [d, J(H,H) = 6.2 Hz, 2 H], 8.05 [d, J(H,H) = 8.3 Hz, 2 H], 7.76 [d, J(H,H) = 8.3 Hz, 2 H], 7.67 [d, J(H,H) = 8.7 Hz, 2 H], 7.47 (m, 7 H), 7.35 [m, J(H,H) = 15.6 Hz, 2 H], 7.15 [d, J(H,H) = 16.2 Hz, 1 H], 2.00 (s, 3 H, -ReCH_3) ppm. ^{13}C NMR (100.6 MHz, $CDCl_3$, 25 °C): δ = 148.2 (2 C), 146.7 (1 C), 140.0 (1 C), 136.1 (1 C), 135.0 (1 C), 134.6 (1 C), 132.0 (2 C), 131.4 (2 C), 130.1 (2 C), 128.4 (1 C), 127.2 (3 C), 126.9 (1 C), 126.5 (2 C), 125.6 (2 C), 125.4 (1 C), 125.2 (2 C), 121.7 (2 C), 24.9 (1 C, -ReCH$_3$) ppm. IR (KBr): $\tilde{\nu}$ = 3434 (w), 3050 (w), 1607 (s), 1592 (m), 1443 (w), 1426 (m), 1412 (w), 1384 (m), 1066 (w), 1015 (m), 969 (w), 931 (vs), 881 (m), 827 (m), 790 (w), 735 (s), 653 (w), 635 (w), 613 (m), 568 (w), 554 (m) cm^{-1}. 541 (m), 422 (w) cm^{-1}. $C_{28}H_{22}NO_3Re$ (606.69): calcd. C 55.41, H 3.66, N 2.31; found C 55.80, H 3.72, N 2.24.

Methyl(4-tolylpyridine)trioxorhenium (13): Yield 67 mg (97%). ^{1}H NMR (400 MHz, $CDCl_3$, 25 °C): δ = 8.31 [d, J(H,H) = 6.2 Hz, 2 H, $NC_2H_2C_2H_2C$-], 7.56 [d, J(H,H) = 6.2 Hz, 2 H, $NC_2H_2C_2H_2C$-], 7.52 [d, J(H,H) = 7.9 Hz, 2 H, -$CC_2H_2C_2H_2CCH_3$], 7.30 [d, J(H,H) = 7.5 Hz, 2 H, -$CC_2H_2C_2H_2CCH_3$], 2.41 (s, 3 H, -PhCH_3), 1.97 (s, 3 H, -ReCH_3) ppm. ^{13}C NMR (100.6 MHz, $CDCl_3$, 25 °C): δ = 151.1 (1 C), 147.1 (2 C), 140.3 (1 C), 133.8 (1 C), 130.0 (2 C), 126.9 (2 C), 122.5 (2 C), 24.8 (1 C, -ReCH$_3$), 21.2 (1 C, Ph-CH$_3$) ppm. IR (KBr): $\tilde{\nu}$ = 33445 (m), 2925 (w), 1610 (s), 492 (m), 1384 (m), 1262 (w), 1227 (w), 12211 (w), 1073 (m), 1037 (w), 1010 (m), 934 (vs), 927 (vs), 854 (w), 811 (s), 721 (m), 559 (m), 498 (m) cm^{-1}. $C_{13}H_{14}NO_3Re$ (418.46): calcd. C 37.31, H 3.37, N 3.35; found C 37.05, H 3.41, N 3.34.

[4-(3,5-Dimethylphenyl)pyridine]methyltrioxorhenium (14): Yield 106 mg (70%). ^{1}H NMR (400 MHz, $CDCl_3$, 25 °C): δ = 8.32 [d, J(H,H) = 6.4 Hz, 2 H, $NC_2H_2C_2H_2C$-], 7.56 [d, J(H,H) = 6.6 Hz, 2 H, $NC_2H_2C_2H_2C$-], 7.21 [s, 2 H, -$CC_2H_2C_2(CH_3)_2CH$], 7.11 [s, 1 H, -$CC_2H_2C_2(CH_3)_2CH$], 2.39 [s, 6 H, -$CC_2H_2C_2(CH_3)_2CH$], 1.98 (s, 3 H, -ReCH_3) ppm. ^{13}C NMR (100.6 MHz, $CDCl_3$, 25 °C): δ = 151.4 (1 C), 147.2 (2 C), 139.0 (2 C), 136.8 (1 C), 131.5 (1 C), 125.0 (2 C), 122.8 (2 C), 24.4 (1 C), 21.3 (2 C) ppm. IR (KBr): $\tilde{\nu}$ = 3434 (w), 2916 (w), 1613 (vs), 1551 (w), 1507 (w), 1408 (w), 1385 (w), 1232 (w), 1073 (m), 1021 (m), 931 (vs), 828 (s), 664 (m), 589 (m), 561 (m), 434 (w), 418 (w) cm^{-1}. $C_{14}H_{16}NO_3Re$ (432.49): calcd. C 38.88, H 3.73, N 3.24; found C 38.88, H 3.73, N 3.24.

Single-Crystal X-ray Structure Determination of Compound 5: $C_{27}H_{19}N$; M_r = 357.43; crystal colour and shape: colourless fragment, crystal dimensions = 0.51 × 0.56 × 0.64 mm; crystal system: monoclinic; space group: Cc (no. 9); a = 14.9971(6), b = 10.9497(4), c = 12.4175(5) Å; β = 114.048(2)°; V = 1862.14(13) Å^3; Z = 4; μ (Mo-K_α) = 0.073 mm^{-1}; $\rho_{calcd.}$ = 1.275 g cm^{-3}; Θ range 2.38–25.34; data collected: 32910; independent data [I_o>2σ(I_o)/all data/R_{int}]: 3360/3397/0.023; data/restraints/parameters: 3397/2/329; $R1$ [I_o>2σ(I_o)/all data] = 0.0255/0.0258; $wR2$ [I_o>2σ(I_o)/all data] = 0.0709/0.0713; GOF = 1.080; $\Delta\rho_{max/min}$ = 0.13/–0.12 e Å^{-3}.

Single-Crystal X-ray Structure Determination of Compound 8: $C_{14}H_{14}NO_3Re$; M_r = 430.47; crystal colour and shape: yellow fragment, crystal dimensions = 0.13 × 0.18 × 0.51 mm; crystal system: monoclinic; space group: $P2_1$ (no. 4); a = 9.0054(2), b = 7.2442(2), c = 11.0721(3) Å; β = 109.3284(11)°; V = 681.60(3) Å^3; Z = 2; μ (Mo-K_α) = 8.916 mm^{-1}; $\rho_{calcd.}$ = 2.098 g cm^{-3}; Θ range 1.95–25.39; data collected: 10806; independent data [I_o>2σ(I_o)/all data/R_{int}]: 2275/2281/0.059; data/restraints/parameters: 2281/1/173;

$R1$ [$I_o > 2\sigma(I_o)$/all data] = 0.0259/0.0259; $wR2$ [$I_o > 2\sigma(I_o)$/all data] = 0.0648/0.0648; GOF = 1.090; $\Delta\rho_{max/min}$ = 2.27/–2.57 e Å^{-3}.

Single-Crystal X-ray Structure Determination of Compound 9: $C_{15}H_{16}NO_3Re$; M_r = 444.49; crystal colour and shape: yellow fragment, crystal dimensions 0.15 × 0.15 × 0.43 mm; crystal system: monoclinic; space group: $P2_1/n$ (no. 14); a = 9.1661(4), b = 7.1741(3), c = 22.3772(9) Å; β = 97.795(2)°; V = 1457.89(11) Å^3; Z = 4; μ (Mo-K_α) = 8.341 mm^{-1}; $\rho_{calcd.}$ = 2.025 g cm^{-3}; Θ range 1.84–25.36; data collected: 29722; independent data [$I_o > 2\sigma(I_o)$/all data/R_{int}]: 2423/2564/0.058; data/restraints/parameters: 2564/0/183; $R1$ [$I_o > 2\sigma(I_o)$/all data] = 0.0289/0.0307; $wR2$ [$I_o > 2\sigma(I_o)$/all data] = 0.0671/0.0680; GOF = 1.261; $\Delta\rho_{max/min}$ = 0.85/–1.54 e Å^{-3}.

Single-Crystal X-ray Structure Determination of Compound 10: $C_{14}H_{13}BrNO_3Re$; M_r = 509.36; crystal colour and shape: yellow fragment, crystal dimensions 0.05 × 0.13 × 0.53 mm; crystal system: triclinic; space group: $P\bar{1}$ (no. 2); a = 5.9849(2), b = 15.9131(6), c = 17.0785(6) Å; α = 66.0608(15), β = 85.8488(15), γ = 86.3720(14)°; V = 1481.68(9) Å^3; Z = 4; μ (Mo-K_α) = 10.903 mm^{-1}; $\rho_{calcd.}$ = 2.283 g cm^{-3}; Θ range 1.31–25.45; data collected: 18921; independent data [$I_o > 2\sigma(I_o)$/all data/R_{int}]: 4839/5188/0.042; data/restraints/parameters: 5188/0/363; $R1$ [$I_o > 2\sigma(I_o)$/all data] = 0.0264/0.0286; $wR2$ [$I_o > 2\sigma(I_o)$/all data] = 0.0697/0.0721; GOF = 1.048; $\Delta\rho_{max/min}$ = 2.13/–1.85 e Å^{-3}.

Single-Crystal X-ray Structure Determination of Compound 11: $C_{20}H_{18}NO_3Re$; M_r = 506.56; crystal colour and shape: yellow fragment, crystal dimensions 0.24 × 0.35 × 0.38 mm; crystal system: triclinic; space group: $P\bar{1}$ (no. 2); a = 5.7288(3), b = 11.4564(6), c = 27.4120(14) Å; α = 82.715(3), β = 89.200(2), γ = 77.895(2)°; V = 1744.74(16) Å^3; Z = 4; μ (Mo-K_α) = 6.983 mm^{-1}; $\rho_{calcd.}$ = 1.929 g cm^{-3}; Θ range 0.75–25.37; data collected: 69973; independent data [$I_o > 2\sigma(I_o)$/all data/R_{int}]: 5347/6039/0.070; data/restraints/parameters: 6039/0/453; $R1$ [$I_o > 2\sigma(I_o)$/all data] = 0.0217/0.0279; $wR2$ [$I_o > 2\sigma(I_o)$/all data] = 0.0507/0.0538; GOF = 1.068; $\Delta\rho_{max/min}$ = 0.87/–0.52 e Å^{-3}.

Single-Crystal X-ray Structure Determination of Compound 12: $C_{28}H_{22}NO_3Re$; M_r = 606.68; crystal colour and shape: yellow fragment, crystal dimensions 0.15 × 0.18 × 0.36 mm; crystal system: triclinic; space group: $P\bar{1}$ (no. 2); a = 9.8694(3), b = 10.9626(4), c = 12.5154(7) Å; α = 99.490(2), β = 105.050(2), γ = 112.906(1)°; V = 1149.44(9) Å^3; Z = 2; μ (Mo-K_α) = 5.316 mm^{-1}; $\rho_{calcd.}$ = 1.753 g cm^{-3}; Θ range 1.77–25.44; data collected: 27800; independent data [$I_o > 2\sigma(I_o)$/all data/R_{int}]: 3917/3955/0.039; data/restraints/parameters: 3955/0/299; $R1$ [$I_o > 2\sigma(I_o)$/all data] = 0.0139/0.0141; $wR2$ [$I_o > 2\sigma(I_o)$/all data] = 0.0356/0.0358; GOF = 1.078; $\Delta\rho_{max/min}$ = 1.12/–0.44 e Å^{-3}.

Single-Crystal X-ray Structure Determination of Compound 13: $C_{13}H_{14}NO_3Re$; M_r = 418.46; crystal colour and shape: yellow fragment, crystal dimensions 0.15 × 0.20 × 0.38 mm; crystal system: monoclinic; space group: $P2_1/c$ (no. 14); a = 11.6924(4), b = 14.3708(4), c = 8.2219(3) Å; β = 110.3695(14)°; V = 1295.13(8) Å^3; Z = 4; μ (Mo-K_α) = 9.381 mm^{-1}; $\rho_{calcd.}$ = 2.146 g cm^{-3}; Θ range 1.86–25.39; data collected: 4902; independent data [$I_o > 2\sigma(I_o)$/all data/R_{int}]: 2196/2260/0.028; data/restraints/parameters: 2260/0/165; $R1$ [$I_o > 2\sigma(I_o)$/all data] = 0.0218/0.0225; $wR2$ [$I_o > 2\sigma(I_o)$/all data] = 0.0556/0.0561; GOF = 1.144; $\Delta\rho_{max/min}$ = 1.12/–1.39 e Å^{-3}.

Single-Crystal X-ray Structure Determination of Compound 14: $C_{14}H_{16}NO_3Re$; M_r = 432.49; crystal colour and shape: yellow needle, crystal dimensions 0.03 × 0.05 × 0.23 mm; crystal system: monoclinic; space group: $P2_1/m$ (no. 11); a = 6.4763(9), b = 11.652(2), c = 18.930(3) Å; β = 93.705(6)°; V = 1425.5(4) Å^3; Z = 4; μ (Mo-K_α) = 8.527 mm^{-1}; $\rho_{calcd.}$ = 2.015 g cm^{-3}; Θ range 1.08–25.37; data collected: 35302; independent data [$I_o > 2\sigma(I_o)$/all data/R_{int}]: 2592/2741/0.048; data/restraints/parameters: 2741/0/195; $R1$ [$I_o > 2\sigma(I_o)$/all data] = 0.0186/0.0200; $wR2$ [$I_o > 2\sigma(I_o)$/all data] = 0.0410/0.0416; GOF = 1.099; $\Delta\rho_{max/min}$ = 1.09/–1.30 e Å^{-3}.

CCDC-777693 (for **5**), -777694 (for **8**), -777695 (**9**), -777696 (for **10**), -777697 (for **11**), -777698 (for **12**), -777699 (for **13**), and -77770 (for **14**) contain the supplementary crystallographic data for this paper. These data can be obtained free of charge from The Cambridge Crystallographic Data Centre via www.ccdc.cam.ac.uk/data_request/cif.

Formation Constant Measurements: An UV/Vis spectrophotometric method was used to determine the formation constants of the chromophoric Lewis base adducts of MTO. Aliquots of a 0.1 mM solution of MTO in CH_2Cl_2 were successively added to a 0.1 mM solution of the ligand in CH_2Cl_2 in a quartz cuvette (path length 1 cm, total volume 3 mL). UV/Vis spectra of the homogeneous solutions at equilibrium containing the metal complex, the ligand and the adduct were recorded in the range of 200–400 nm before and after each addition of the MTO aliquot. The values of the formation constants were calculated by fitting the equilibrium absorbance at a certain wavelength to Equation (2) or (3) according to the chosen wavelength and the free ligand absorption using the IGOR computer program.

Catalysis: In a typical experiment, 1-octene (0.628 mL, 4 mmol), MTO (10 mg, 0.04 mmol), ligand (0.2 mmol), 0.200 mL of mesitylene (internal standard), 0.200 mL of toluene (internal standard) and 2.45 mL of CH_2Cl_2 were added to the reaction vessel under standard conditions at room temperature. The reaction started upon addition of H_2O_2 (35% aqueous solution) (0.55 mL, 6 mmol) under vigorous stirring. The course of the reaction was monitored by quantitative GC analysis. Samples (0.2 mL) were taken at specific time intervals, treated with Na_2SO_3 to quench the excess of peroxide and to remove water, filtered and diluted with dry CH_2Cl_2 before injection into a GC column. The conversion of 1-octene and the formation of octene epoxide were calculated from calibration curves (r^2 = 0.999) recorded prior to the reaction course.

Testing the Photostability of the Complexes: Selected ligands were treated with an equimolar amount of ^{17}O-labelled MTO (prepared by a published procedure[31]) or in a fivefold excess and the ^1H and ^{17}O NMR spectra were recorded. The adduct solutions (0.1 M in $CDCl_3$) were then exposed to UV light and analysed again by ^1H and ^{17}O NMR spectroscopy. For the UV/Vis analysis, a 0.1 M solution of complex **11** in CH_2Cl_2 was prepared and exposed to UV light. Samples were taken over a timespan of 2 h, diluted with CH_2Cl_2 and the UV/Vis spectra were recorded.

Supporting Information (see also the footnote on the first page of this article): UV/Vis spectra of ligands and complexes, spectroscopic data for the determination of the stability constants and ^{17}O NMR spectra of selected complexes.

Acknowledgments

S. A. H. thanks the Bavarian elite network NanoCat for a Ph. D. grant and for financial support of the project.

[1] R. I. Beattie, P. J. Jones, *Inorg. Chem.* **1979**, *18*, 2318–2319.
[2] W. A. Herrmann, J. G. Kuchler, J. K. Felixberger, E. Herdtweck, W. Wagner, *Angew. Chem.* **1988**, *100*, 420–422; *Angew. Chem. Int. Ed. Engl.* **1988**, *27*, 394–396.
[3] F. E. Kühn, A. Scherbaum, W. A. Herrmann, *J. Organomet. Chem.* **2004**, *689*, 4149–4164.

[4] W. A. Herrmann, M. Wang, *Angew. Chem.* **1991**, *103*, 1709–1711; *Angew. Chem. Int. Ed. Engl.* **1991**, *30*, 1641–1643.
[5] W. A. Herrmann, W. Wagner, U. N. Flessner, U. Volkhardt, H. Komber, *Angew. Chem.* **1991**, *103*, 1704–1706; *Angew. Chem. Int. Ed. Engl.* **1991**, *30*, 1636–1638.
[6] J. E. Ziegler, M. J. Zdilla, A. J. Evans, M. M. Abu-Omar, *Inorg. Chem.* **2009**, *48*, 9998–10000.
[7] W. A. Herrmann, R. W. Fischer, D. W. Marz, *Angew. Chem.* **1991**, *103*, 1706–1709; *Angew. Chem. Int. Ed. Engl.* **1991**, *30*, 1638–1641.
[8] J. Rudolph, K. L. Reddy, J. P. Chiang, K. B. Sharpless, *J. Am. Chem. Soc.* **1997**, *119*, 6189–6190 and references cited therein.
[9] F. E. Kühn, A. M. Santos, W. A. Herrmann, *Dalton Trans.* **2005**, 2483–2491 and references cited therein.
[10] C. Copéret, H. Adolfson, K. B. Sharpless, *Chem. Commun.* **1997**, 1565–1566.
[11] W. A. Herrmann, H. Ding, R. M. Kratzer, F. E. Kühn, J. J. Haider, R. W. Fischer, *J. Organomet. Chem.* **1997**, *549*, 319–322.
[12] W. D. Wang, J. H. Espenson, *J. Am. Chem. Soc.* **1998**, *120*, 11335–11341.
[13] W. A. Herrmann, R. M. Kratzer, H. Ding, W. R. Thiel, H. Glas, *J. Organomet. Chem.* **1998**, *555*, 293–295.
[14] H. Adolfsson, A. Converso, K. B. Sharpless, *Tetrahedron Lett.* **1999**, *40*, 3991–3994.
[15] F. E. Kühn, A. M. Santos, P. W. Roesky, E. Herdtweck, W. Scherer, P. Gisdakis, I. V. Yudanov, C. Di Valentin, N. Rösch, *Chem. Eur. J.* **1999**, *5*, 3603–3615.
[16] C. Copéret, H. Adolfson, J. P. Chiang, A. K. Yudin, *J. Org. Chem.* **2000**, *65*, 8651–8658.
[17] P. Ferreira, W. D. Xue, É. Bencze, E. Herdtweck, F. E. Kühn, *Inorg. Chem.* **2001**, *40*, 5834–5841.
[18] M. J. Sabater, M. E. Domine, A. Corma, *J. Catal.* **2002**, *210*, 192–197.
[19] P. Altmann, F. E. Kühn, *J. Organomet. Chem.* **2009**, *694*, 4032–4035.
[20] H. Kunkely, T. Türk, C. Teixeira, C. de Meric de Bellefon, W. A. Herrmann, A. Vogler, *Organometallics* **1991**, *10*, 2090–2092.
[21] W. A. Herrmann, F. E. Kühn, D. A. Fiedler, M. R. Mattner, M. R. Geisberger, H. Kunkely, A. Vogler, S. Steenken, *Organometallics* **1995**, *14*, 5377–5381.
[22] H. Kunkely, A. Vogler, *J. Photochem. Photobiol. A: Chem.* **1996**, *94*, 135–138.
[23] H. Kunkely, A. Vogler, *J. Photochem. Photobiol. A: Chem.* **1997**, *103*, 227–229.
[24] M.-D. Zhou, S.-L. Zang, E. Herdtweck, F. E. Kühn, *J. Organomet. Chem.* **2008**, *693*, 2473–2477.
[25] P. Wikrent, B. J. Drouin, S. G. Kukolich, J. C. Lilly, M. T. Ashby, W. A. Herrmann, W. Scherer, *J. Chem. Phys.* **1977**, *107*, 2187–2192.
[26] A. M. Al-Ajlouni, A. Günyar, M.-D. Zhou, P. N. W. Baxter, F. E. Kühn, *Eur. J. Inorg. Chem.* **2009**, 1019–1026.
[27] M. Y. Shatnawi, A. M. Al-Ajlouni, *Jordan J. Chem.* **2009**, *4*, 119–130.
[28] S. M. Nabavizadeh, *Inorg. Chem.* **2003**, *42*, 4204–4208.
[29] S. M. Nabavizadeh, *Dalton Trans.* **2005**, 1644–1648.
[30] S. M. Nabavizadeh, A. Akbari, M. Rashidi, *Eur. J. Inorg. Chem.* **2005**, 2368–2375.
[31] S. Yamazaki, *Org. Biomol. Chem.* **2007**, *5*, 2109–2113.
[32] W. A. Herrmann, F. E. Kühn, P. W. Roesky, *J. Organomet. Chem.* **1995**, *485*, 243–251.
[33] W. A. Herrmann, F. E. Kühn, M. U. Rauch, J. D. G. Correia, G. Artus, *Inorg. Chem.* **1995**, *34*, 2914–2920.
[34] E. Tosh, H. K. M. Mitterpleininger, A. M. J. Rost, D. Veljanovski, W. A. Herrmann, F. E. Kühn, *Green Chem.* **2007**, *12*, 1296–1298.
[35] V. Aranyos, J. Hjelm, A. Hagfeldt, H. Grennberg, *J. Chem. Soc., Dalton Trans.* **2001**, 1319–1325.
[36] N. Kudo, M. Perseghini, G. C. Fu, *Angew. Chem. Int. Ed.* **2006**, *45*, 1282–1284.

Received: March 29, 2010
Published Online: July 23, 2010

